Journal of Chromatography A, 1461 (2016) 70–77

Contents lists available at ScienceDirect

Journal of Chromatography A

journal homepage: www.elsevier.com/locate/chroma

Residual on column host cell protein analysis during lifetime studies of protein A chromatography

Katherine Lintern[a], Mili Pathak[b], C. Mark Smales[c], Kevin Howland[c], Anurag Rathore[b], Daniel G. Bracewell[a,*]

[a] Department of Biochemical Engineering, University College London, Bernard Katz Building, Gordon Street, London WC1H 0AH, United Kingdom
[b] Department of Chemical Engineering, IIT Delhi, Hauz Khas, New Delhi, Delhi 110016, India
[c] Centre for Industrial Biotechnology, School of Biosciences, University of Kent, Canterbury, CT2 7NJ, United Kingdom

ARTICLE INFO

Article history:
Received 9 February 2016
Received in revised form 16 July 2016
Accepted 20 July 2016
Available online 21 July 2016

Keywords:
Protein A affinity chromatography
Host cell proteins
LC–MS/MS
Resin ageing
Process-related impurities
Bioprocessing

ABSTRACT

Capacity reduction in protein A affinity chromatography with extended cycling during therapeutic antibody manufacture is well documented. Identification of which residual proteins remain from previous cycles during the lifetime of these adsorbent materials is required to understand their role in this ageing process, but represents a significant metrological challenge. Scanning electron microscopy (SEM) and liquid chromatography mass spectrometry (LC–MS/MS) are combined to detect and map this phenomenon of protein carry-over. We show that there is a morphological change at the surface of the agarose resin, revealing deposits on the polymer fibres increasing with cycle number. The amount of residual host cell proteins (HCPs) by LC–MS/MS present on the resin is shown to increase 10-fold between 50 and 100 cycles. During this same period the functional class of the predominant HCPs associated with the resin increased in diversity, with number of proteins identified increasing 5-fold. This ageing is observed in the context of the product quality of the eluate HCP and protein A leachate concentration remaining constant with cycle number.

1. Introduction

Monoclonal antibody (mAb) production is the largest sector of the biopharmaceutical industry and protein A chromatography provides the core purification operation for the robust manufacture of these products [1]. The upstream elements of these processes have incrementally improved since their emergence as an important class of medicines to now generate feedstock material with far higher IgG titres (up to 10 g/l). This has subsequently placed an increased strain on downstream processes for mAb purification, due to an associated challenge from elevated levels of process related impurities [2]. The refinement of affinity chromatography resins has helped manage these challenges, incorporating modified protein A ligands and improved matrix structure to enable the extended use of the resins as they show improved stability across a greater range of pH. Consequently, harsher cleaning conditions have commonly been adopted to reduce fouling and prolong the lifetime of the expensive protein A resin.

Chromatography columns can and do still lose productivity and fail, with diagnostic faults including a reduction in dynamic binding capacity, pressure build-ups and a decrease in HCP clearance. Furthermore, the accumulation of material of host cell origin on the resin is observed, particularly with resin cycled many times. This fouling phenomenon has been correlated with reduced column productivity, and also poses a potential purity and safety risk to the mAb product [3]. The safety concerns particularly relate to impurities that may be found at elevated levels post protein A chromatography. Recently, the application of mass spectrometry has enabled identification of specific HCP species [4–7] as they pass through the protein A chromatography step, increasing knowledge of associated risks beyond that achieved with conventional ELISA approaches which provide summative measure of all HCPs. Following this success it is logical that mass spectrometry might be used to identify trends and commonalities in residual HCPs during a chromatography columns lifetime.

It has been demonstrated that fouling is a cumulative process [8,9], often affecting mass transfer into the resin bead, where pore blockage by histones [10,11] and destabilised mAb complexes have been reported as causative agents [12,13]. Such findings highlight the need for a better process understanding of fouling over the lifetime of resin use. Process conditions, including the low pH elution

* Corresponding author.
E-mail address: d.bracewell@ucl.ac.uk (D.G. Bracewell).

http://dx.doi.org/10.1016/j.chroma.2016.07.055

step and the high pH cleaning-in-place (CIP), have been demonstrated to affect protein structure and stability [14] and are thought to contribute to the precipitation of HCP and mAbs onto the resin. The use of these harsh conditions, most notably NaOH, is a prerequisite to control bioburden, a concern when resins are in use for a period of months.

Studies have also been undertaken to screen for conditions that reduce protein fouling and increase resin lifetime [15], but are limited in that they do not address the dynamics of fouling with respect to resin cycling. Furthermore, although previous studies have provided some insight into which species can potentially foul the protein A resin, these studies have not extended to understanding the progression of fouling up to the high number of cycles relevant to the expectations and requirements of commercial processes [16]. This is of particular relevance, as the high relative cost of protein A resin necessitates resin re-use [14,17]. This study reveals how the residual material deposited on the chromatographic resin under repeated cycling over its lifetime is associated with changes in separation performance, focussing on the HCP components contributing to this progressive effect.

2. Materials and methods

2.1. Generation of fouled resin

Clarified CHO cell feed material (viability at harvest >99%) contained an IgG1 mAb at 1.7 mg/ml and was donated from an industrial source. Feed material was stored at −70° C and centrifuged at 4630*g* for 15 min and passed first through a 0.5 μm and then a 0.22 μm filter (Supor, Pall) prior to use to remove any precipitates.

Generation of fouled MabSelect SuRe (GE Healthcare, Hatfield, UK) resin was achieved by packing 3 ml columns (5 mm × 160 mm) for 100 cycles and 60 cycles and 1 ml columns (5 mm × 50 mm) for 80 cycles and 50 cycles and applying CHO cell culture. The decrease in DBC and yield was found to be comparable between the column sizes when a constant linear flow velocity is used, thus qualifying the use of a smaller column to conserve feed material. Chromatography was performed using an AKTA® Purifier (GE Healthcare Life Sciences, Stockholm, Sweden) as follows: MiliQ water wash (5 CV) followed by equilibration with 20 mM Tris, 100 mM NaCl pH 7.4 (4 CV, 500 cm/h). Feed material was loaded to 15.3 mg mAb/ml resin and run at 500 cm/h before a washing step again with 20 mM Tris, 100 mM NaCl pH 7.4 (7 CV, 500 cm/h). Elution was with 100 mM acetic acid pH 3.4 (5 CV, 250 cm/h) after which the column was striped using 2 M NaCl (3 CV, 500 cm/h)/h). Cleaning in place (CIP) was performed with 50 mM NaOH, 1 M NaCl, contact time being maintained below 16 min. The sequence for cycles and CIP regimes was as follows: Cycle 1–3; CIP; Cycle 4–6; CIP; Cycle 7–9; CIP; Cycle 10; Blank run; Cycle with purified IgG for measurement of dynamic binding capacity; CIP. This sequence was used for every group of 10 cycles. Columns were run for 50, 60, 80 and 100 cycles and resin samples taken and stored in 20% ethanol at 4° C prior to analysis.

2.2. Determination of DBC

Dynamic binding capacity (DBC) at 10% breakthrough was determined at a linear flow rate of 500 cm/h. The column was equilibrated with 5 CV of 20 mM phosphate buffer pH 6.2 with 50 mM NaCl (equilibration buffer). The UV monitor was auto zeroed. Purified IgG 1 mAb was loaded at 15.3 mg/ml resin until the breakthrough was obtained and continued until saturation was reached. The saturation of the breakthrough curve indicated that the antibody concentration on entering the UV monitor was identical to the antibody concentration in the feed. The dynamic binding capacity was determined using the following calculation:

$$D_{10\%} = \frac{(V_{10\%} - V_0)\,C_0}{V_c}$$

Where $D_{10\%}$ = dynamic binding capacity at 10% of breakthrough curve (mg of mAb/ml of resin), C_0 = antibody concentration (mg/ml), V_c = geometric total volume (ml), and V_0 = void volume (ml).

The DBC values were normalized using the equation:

$$ND_{10\%} = \frac{D_{10\%}\text{at}i^{\text{th}}\text{cycle}}{D_{10\%}\text{at}0^{\text{th}}\text{cycle}} \times 100$$

Where, $ND_{10\%}$ = normalized dynamic binding capacity at 10% of breakthrough curve (%), i = intermediate cycle.

2.3. LC–MS/MS

2.3.1. HCP digestion and removal from protein A resin

Initially, 50 μl resin (100 μl 50% slurry) was suspended in 50 μl 8 M urea, 100 mM ammonium carbonate. Next, 2 μl 450 mM dithiothreitol was added and the mixture incubated at room temperature for one hour. This was followed by incubation with 20 μl of 100 mM iodoacetamide for 15 min at room temperature to achieve carbidomethylation of the sample. Urea was diluted by the addition of 128 μl MiliQ water prior to incubation at 37° C for 1 h with 5 μg modified sequence grade trypsin (Promega, Southampton, UK).

2.3.2. Liquid chromatography (LC)

Samples were applied to a C_{18} Acclaim PepMap100 (Thermo, UK) 75 μm internal diameter x 15 cm (C_{18}, 3 μm, 100A) for on-line reverse phase HPLC (NanoLC Ultimate3000, Thermo UK). Elution was performed with a linear acetonitrile gradient (solvent A = 0.05% TFA, solvent B = 0.05% TFA, 90% acetonitrile) in a 40 min cycle at a flow rate of 300 nl/min. LC was coupled to a fraction collector (Proteineer fcII, Bruker, Coventry, UK), dividing eluates into 120 fractions and mixing with matrix solution (α-cyano-4-hydroxycinnamic acid (CHCA), Sigma UK, reconstituted according to manufacturer's guidelines in 89% acetonitrile, 0.1% TFA) prior to being spotted onto a MALDI-ToF target plate (MTP AnchorChip600 384 T F, Bruker, Coventry, UK).

2.3.3. Mass spectrometry

MALDI-TOF-TOF was conducted using an UltrafleXtreme MALDI-TOF instrument (Bruker, Coventry, UK) in positive ion reflector mode and 50% laser power and MS-MS was conducted on the ten most intense peaks for each target spot. Generated peptide masses with an ion score exceeding the threshold set for $p < 0.05$ were interrogated using the Mascot algorithm (matrixscience.com) to search all taxonomies in the SwissProt database. Search parameters were 547599 sequences analysed in the selected database, fixed modifications: carbidomethyl (C); variable modifications: oxidation (M); mass values: monoisotopic; protein mass: unrestricted; peptide mass tolerance: +/− 50 ppm; fragment mass tolerance: +/− 0.5 Da; instrument: MALDI-TOF-TOF.

2.4. Electron microscopy

2.4.1. Sample preparation

Resin samples were rinsed twice in distilled water before fixing with 20% glutaraldehyde for 20 min, followed by two further water rinses and staining with 1% osmium tetroxide for 20 min. Resin samples were then dehydrated through an incremental 0–100% ethanol gradient in preparation for critical point drying, which was performed using a E3100 chamber dryer (Quorum Technologies).

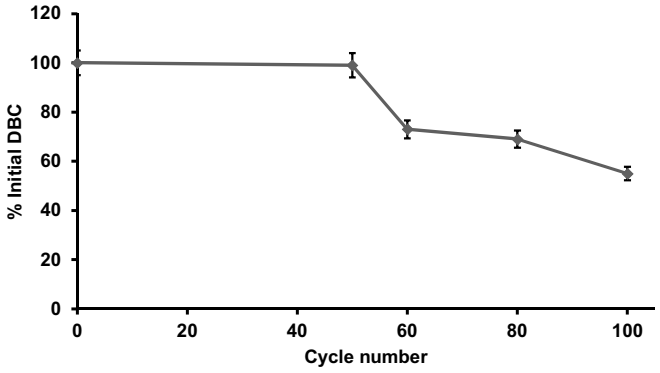

Fig. 1. Dynamic binding capacity (DBC) at 10% breakthrough of cycled resin. The DBC was calculated for resin which had undergone 50, 60, 80 and 100 cycles with IgG spiked feedstock material, and expressed as mg of IgG per ml of resin. Error bars represent average percentage error derived from standard curve data points (n = 3).

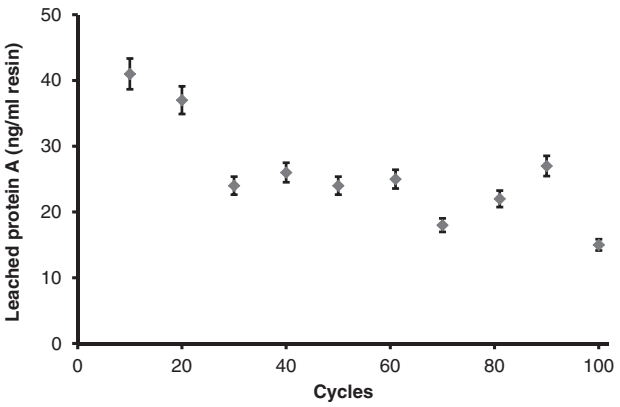

Fig. 2. Amounts of leached protein A from cycled resin. Column flow through samples from every 10th cycle for a total of 100 cycles were assayed for leached protein A. Error bars denote average percentage error from standard curve values (n = 3).

Once completely dry, resin beads were transferred to carbon coated stubs and gold coated with an ion beam coater (Gatan Model 681, Oxford, UK) at 6 mA and an acceleration voltage of 10 keV to a thickness of 2–3 nm.

2.4.2. Microscopy

Images were obtained using a Jeol JSM-7401F field emission scanning electron microscope (Jeol Ltd, Tokyo, Japan). Parameters for image acquisition were 2 kV accelerating voltage and 5.0 μA, with a working distance of 5 mm.

2.5. Immunoassays

2.5.1. Leached protein A

Protein A leachate was measured in the eluate from every 10th chromatographic cycle using Dip and Read™ Residual Protein A Detection Kit (Pall Life Sciences, Portsmouth, UK) using an Octet Red 384 instrument (ForteBio, Pall Life Sciences, CA).

2.5.2. HCP ELISA

Total eluate HCP was measured by analysing samples every ten cycles using the commercially available 3rd Generation Cygnus CHO HCP ELISA kit (F550) as per the manufacturer's guidelines (Cygnus Technologies, Southport NC).

3. Results & discussion

3.1. Functional capacity of cycled MabSelect SuRe

Fig. 1 demonstrates that there is a reduction in dynamic binding capacity (DBC) with increasing cycle number. To investigate whether this reduction in DBC was attributable to a loss of protein A ligand, the amounts of leached protein A were monitored (Fig. 2). No trend in leachate was observed with increased cycle number; although variable, protein A appeared to leach at a relatively constant amount at each cycle. This is in line with published data for MabSelect SuRe [18], which indicates ligand loss is unlikely to be the cause of the observed significant loss inn capacity. There was no relationship observed between cycle number and the HCP content of the eluate (Fig. 3), with the observed HCP concentration falling between 130 and 370 ng/ml throughout the study period. The variance seen in these key impurities during the lifetime studies though wide is representative of that seen in other studies [14,18].

3.2. Visualisation of the fouling phenomenon on the resin surface

Protein A resin samples from columns were prepared for electron microscopy in order to observe the surface topography. Critical point drying was selected for sample preparation as it is a method developed for the preservation of biological samples and should thus maintain the surface structures. A limitation of this approach is that some features may have been lost due to the preparation methods (e.g. lipid leaching through the ethanol dehydration steps). However, the method provides the best known means to preserve the resin surface and minimise additional process artefacts in order to study how mAb and HCPs evolve over extended cycling.

The resulting images shown are representative of each sample, although inter-sample heterogeneity was observed between resin beads, a phenomenon also described by others [12,15]. This may be the result of the different degrees of resin fouling occurring with respect to the variations in the position of the resin within the chromatographic column, as described in similar purification systems [19]. In order to remove or minimise this effect the contents of the column were mixed upon column unpacking to ensure that a subsample representative of the overall extent of fouling in the column was obtained.

Resin exposed to a greater number of cycles (100 cycles, Fig. 4D) was seen to have more accumulated surface fouling than resin from lower cycle numbers. This manifested both as surface structures and inter-matrix deposits (Fig. 4). While identity of the accumulated matter cannot be deduced from images alone, the extent of the deposits increases with cycle number. It is likely therefore that

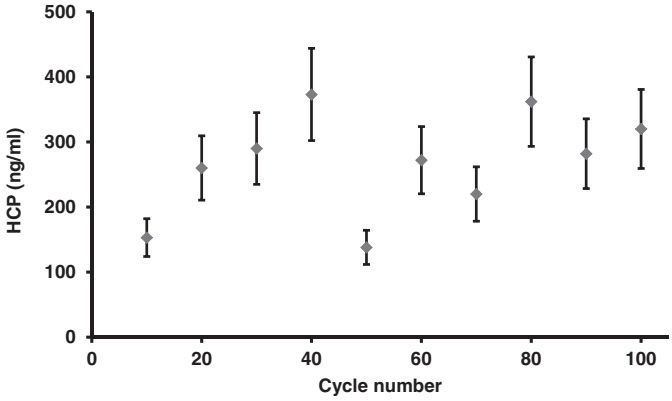

Fig. 3. Typical host cell protein (HCP) content in the protein A eluent. HCP concentrations are expressed as ng per ml of eluent (all <10 ppm). Error bars represent average perecentage error, calculated from standard curve data (n = 3).

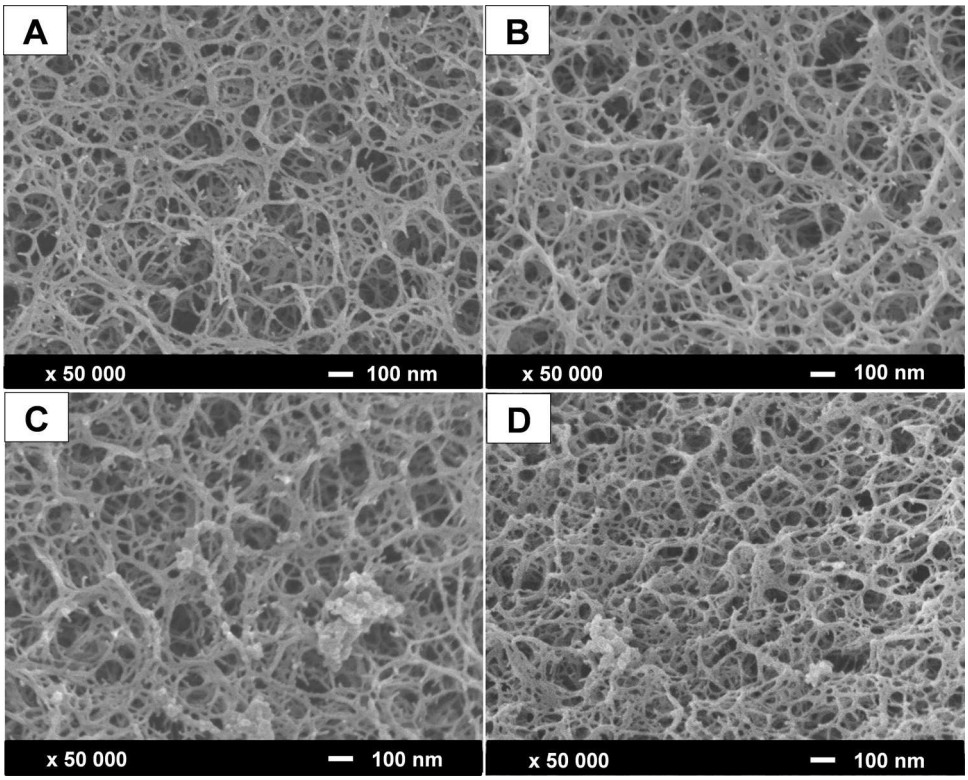

Fig. 4. Scanning electron microscopy images of the protein A resin surface. A) Unused MabSelect SuRe, B) MabSelect SuRe after 50 cycles, C) 60 cycles and D) 100 cycles at x50 000 magnification.

this material is derived from the feedstock and so can be considered as foulant in the form of process and product related impurities. The variety of structures, ranging from small globular deposits, inter-fibre films and larger, more complex structures implies a progressive fouling phenomena and a degree of heterogeneity. This heterogeneity may be dependent on the position and orientation of the resin within the packed bed as has been seen in confocal microscopy based studies of chromatography fouling [13]. This observation of accumulation of material on the resin coincides with an associated increase in HCP detected by LC–MS/MS as discussed in the following sections.

3.3. Profile of residual host cell protein on cycled resin

This investigation focussed on the contribution of host cell proteins (HCP) to the physical effects of fouling. No trend was observed in the quantity of HCP in the eluate over successive cycles (Fig. 3), although others have shown a reduction of HCP in the eluate during the first 50 cycles [18].

Prior to LC–MS/MS, resin samples were incubated in strong reducing conditions (8 M urea, 100 mM ammonium carbonate, 2 mM dithiothreitol) to promote the effective removal of proteinaceous deposits from the agarose matrix. Tryptic digestion of these proteins followed and the peptide suspension was applied to a reverse phase HPLC column coupled to a sample spotter, generating 120 spots per sample, enabling greater resolution of peptide fragments in preparation for MALDI-TOF tandem mass spectrometry analysis. This LC–MS/MS approach is recognised as an emerging orthogonal technology for the identification of HCPs [3] and in this study enabled identification of in excess of 800 peptide fragments from cycled resin samples.

The accumulation of material on the resin, as demonstrated by SEM, coincides with the increasing number of peptides assigned to HCPs detected by LC–MS/MS. A positive correlation was observed between the number of times a HCP was identified from its peptide fragments and the number of cycles to which the resin sample had been subjected (Fig. 5).

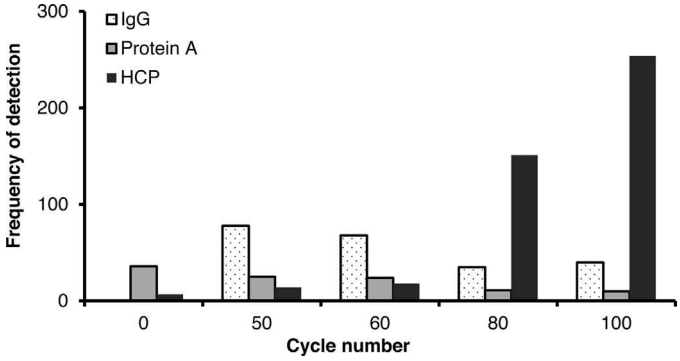

Fig. 5. Trend in IgG and HCP contribution to the number of peptides identified from the surface of cycled protein A resin. Data was acquired from LC–MS/MS analysis of resin samples which had been cycled with clarified CHO feed material for 50, 60, 80 or 100 chromatographic cycles. Each statistically relevant protein identification from MS/MS analysis of peptides was included. "HCP" refers to all identified proteins other than protein A, IgG and analytical contaminants (human keratin and porcine trypsin).

This relationship does not appear to be linear, with the sharpest rise in identified peptides occurring between 60 and 80 cycles. Of note, in conjunction with the increase in total peptides detected, a progressive reduction in the number of mAb and protein A fragments observed was seen with increased cycle number resin. It is interesting that the proportion of mAb decreases with increasing cycle number; further investigation is required to understand whether this can be attributed to a direct interaction between mAb and HCPs or simple displacement. The data suggests a mechanism by which not only the relative amount of HCP carried over from

Table 1
Categorisation of proteins removed from protein A resin identified by LC–MS/MS. Proteins were identified from their corresponding peptide fragments detected by LC–MS/MS and classified according to their primary cellular function derived from data published on the UniProt digital repository. Protein identifications were counted for each resin sample over the 120 fractions generated.

	Cytoskeletal	Protein synthesis	Protein modification	Histone	Extracellular matrix	Homeostasis	Chaperone	Metabolism	Proteolysis	Trafficking	IgG	Protein A	Undefined protein	TOTAL
–	2	0	0	0	0	1	0	2	0	0	0	36	2	43
50	2	7	0	1	0	0	1	1	0	2	78	25	0	117
60	2	8	0	2	0	0	0	4	0	2	68	24	0	110
80	39	37	8	1	10	2	20	30	0	4	35	11	0	197
100	78	44	14	0	18	4	32	52	3	9	40	10	0	304

each cycle increases, but also the diversity of the HCPs carried over as cycle number increases (Table 1).

3.4. Residual HCP dynamics with cycle number

In order to facilitate the identification and interpretation of any trends in abundance and profile of HCPs, proteins were grouped according to their published UniProt primary in vivo role. It was deemed insufficient to monitor protein abundancy without attempting to understand why, if at all, some proteins have a higher tendency to be present and be more abundant in the foulant layer. Categorisation of the peptides identified according to their broad functional class and their relative abundance is shown in Table 1. The majority of peptides detected were of eukaryotic origin and there was no significant rise in prokaryotic peptides detected at higher cycle number samples, which may have been associated with bioburden.

The HCP component profile differed between resin cycles (Fig. 6) and the increase in total protein on high cycle number resin is not simply the result of linear accumulation of residual HCPs due to increased exposure time. Where that so, a much higher proportion of the HCP detected would be expected to be common between resin samples, contrary to the data depicted in Table 1.

Grouping the HCPs by functional class enabled a comparison to be made in HCP composition of fouled resin samples, and this data is summarised in Fig. 7. Protein A and IgG formed a greater proportion of proteins identified from peptides detected on resin cycled 50 and 60 times than for resins from higher number of cycles. Fig. 7 shows that above 60 cycles there was a shift in the relative proportion of protein groups, with the decrease in protein A and IgG coinciding with a greater representation of cytoskeletal, chaperone and metabolic and protein synthesis related proteins.

There was a dramatic change in HCP composition between 60 and 80 cycles when the total number of protein identifications, and the variety of proteins detected, rose sharply (Fig. 7). Metabolic enzymes and protein synthesis related proteins, while also detected at the lower cycle numbers, increased in proportion with extended cycle number. Other functional classes were seen to also contribute to total HCP load, significantly chaperones, cytoskeletal and extracellular matrix components (Fig. 4). These classes of protein are known to be abundant in CHO cells, and so would be expected in relatively high concentrations in the host cell feedstock if the harvest unit operations were insufficient to remove them from the HCCF prior to application on the chromatography column. Overall this suggests a critical point occurs in fouling as HCPs begin to accumulate at around 50 cycles in this study whereupon a greater diversity of HCPs progressively bind.

There is evidence that proteases in the feedstock can contribute to a decline in the performance of protein A chromatography [16,20]. It can result in degradation of the ligand [20], product proteolysis during processing l [21,22] or subsequently in the purified product if they are not adequately cleared [23]. Proteases comprised a small proportion of the total proteins identified from fouled resin (Table 1) and were found only in the 100 cycle sample (Table 2). This confirms that under these experimental conditions proteases were present in the feed material and contributed to fouling of the resin, although whether such proteases retained proteolytic activity once adhered to the resin is uncertain.

3.5. Linking the observed HCP profile to protein A resin performance

Fig. 2 revealed the amount of protein A leachate was within a range between 15 and 41 ng/ml, indicating a relatively constant level of leaching with cycle number. Interestingly, MS/MS data of the material remaining on the resin appears to reveal that fewer peptides attributable to protein A fragments were present with increasing cycle number (Table 1, Fig. 6). This gradual decrease is confounded by the far greater increase in monoclonal antibody and HCP peptides (Fig. 5). As detection of protein A leachate was low it is unlikely that a loss of protein A is solely responsible for the observed reduction in DBC. The data indicates that an increase in residual HCP is associated with reduced DBC.

Additionally, residual IgG was detected from early cycles and may reduce DBC by blocking protein A binding sites for the next cycle of mAb, and could also act as a nucleus/catalyst for additional HCP binding. HCP mediated obscuration of ligand and mass transfer issues may play a role, although the specific location and nature of foulant material falls beyond the scope of this study.

The apparent correlation between the reduction in DBC and the accumulation of residual HCP measured by mass spectrometry may be indicative of the onset of fouling which CIP is not effective against. This nonlinear phenomenon takes hold after approximately 60 cycles in this case and is corroborated by the morphological observations under electron microscopy at the resin surface where significant deposits are observed at 100 cycles.

3.6. Implication of accumulated HCP profile on product purity

Table 2 lists the proteins which were identified from peptides yielded from the majority of cycled resin samples. Although not necessarily the most frequently detected peptides, eight of the corresponding proteins were identified in at least three out of four of the cycled resins. The diversity of proteins was found to increase dramatically after 60 cycles (Fig. 5), yet these “core” proteins were still found at higher cycle numbers.

That these were persistently observed raises some interesting points for discussion, particularly when it is considered that there are commonalities between the residual proteins identified here and proteins which have been reported by others to associate and elute with the mAb product (it should be noted the data in these studies is typically from new protein A resin). Such proteins include actin [5,7,24], heat shock proteins [4,5,7,24], elongation factors [4,7], peroxiredoxin [5,7,24–26] enolase [5], phospholipases [24], glyceraldehyde-3-phosohate dehydrogenase [7,24], E1 ubiquitin related proteins [25] and hypoxia upregulated protein 1 [25]. A basis for this frequently identified subset of the CHO proteome which are more likely to find their way through protein A purification is yet to

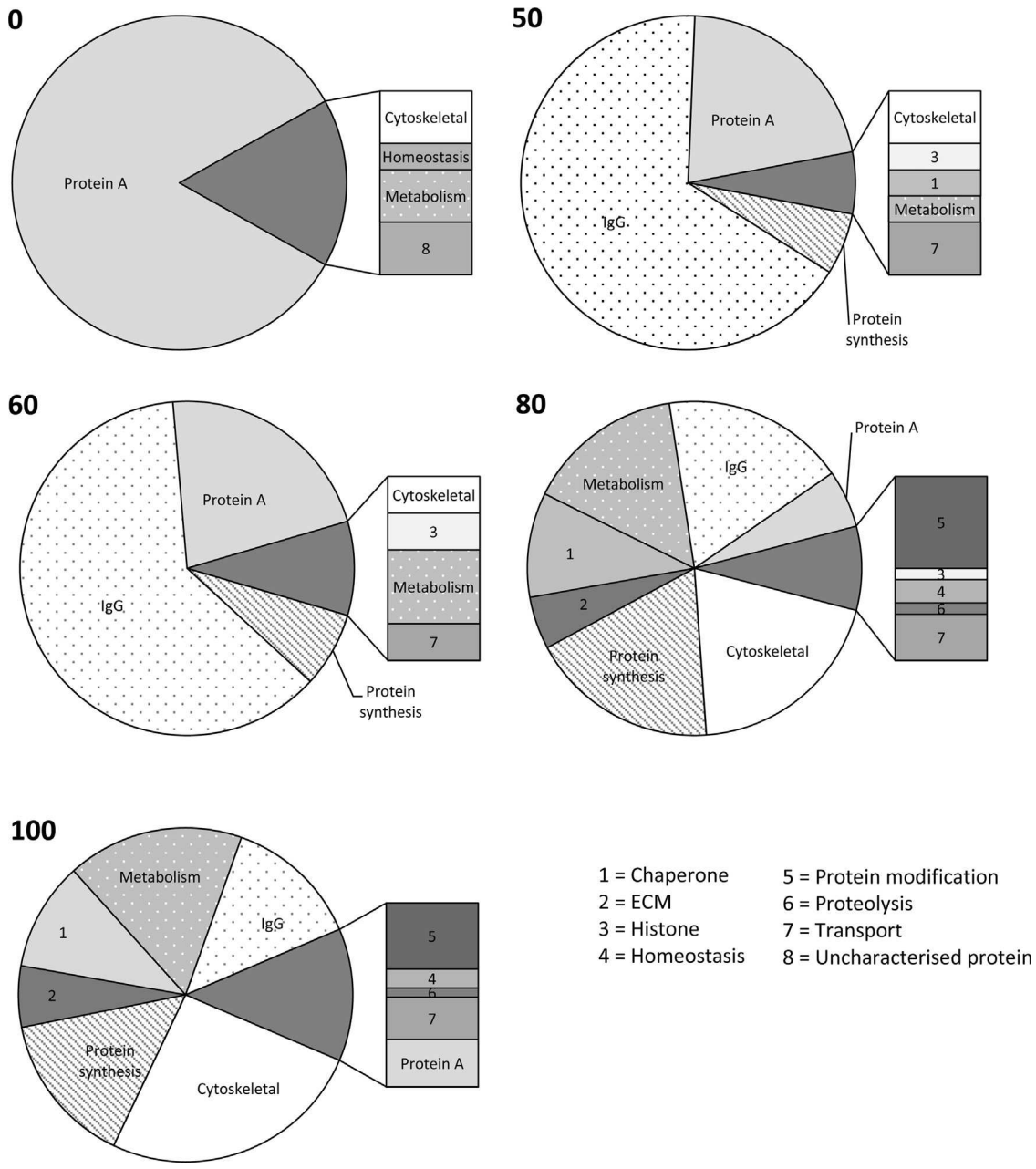

Fig. 6. Proportion of residual proteins removed from protein A resin cycled for 50, 60, 80 and 100 cycles and the blank (0). The blank was run in the absence of feed material with purified IgG to determine the DBC of the uncycled resin. Identified proteins were grouped according to their cellular function and groups plotted as the percentage of total proteins identified from their peptide fragments detected by LC–MS/MS. Protein groups comprising less than 4% of total detected proteins are combined into one section of the pie chart and shown in an adjacent sub-chart.

emerge. The subset found here is diverse in terms of biological and physicochemical properties. This diversity increases as fouling proceeds becoming apparently increasingly non-specific. Nevertheless understanding of these species could be put to use in targeted HCP assays e.g. toward those found to accumulate during the protein A column's lifetime thereby mitigating associated risks. Identification of strategies to reduce the chromatography feedstock concentration of such proteins or disrupt their on-column interactions may provide further benefits.

3.7. The involvement of multiple species in resin ageing

In this study one class of process related impurity was investigated, HCPs. Although a highly varied class in itself, during protein A chromatography HCPs are present alongside a wide range of product and process related impurities of diverse sizes and physicochemical properties. The work of others points to several of these impurities, including chromatin [10,24,25], product (mAb) complexes [12] and lipids [9], playing a role in ageing. Here, the focus is on the change in protein cohort over time to better address questions of process risks for HCPs which are typically regarded as critical quality attributes for antibody therapeutics.

A full understanding of ageing and fouling is only likely to occur when interactions between species can be accounted for e.g. interactions between HCPs and chromatin or HCPs and the product. All of these components are labile and may be damaged/unfolded during processing. Any such species will further increase complexity, perhaps providing sites for fouling and the heterogeneity that can be observed under electron microscopy.

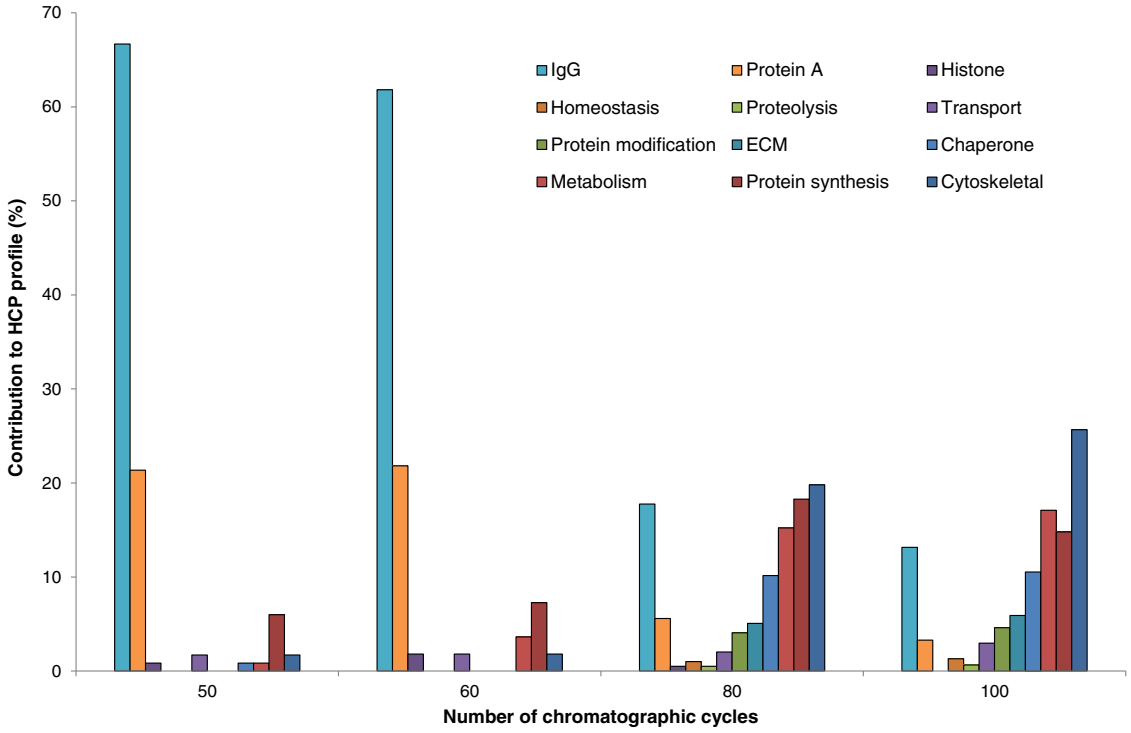

Fig. 7. Relative proportion of each protein group in the profile of residual protein removed from resin cycled 50, 60, 80 and 100 times. The identity of proteins was determined from the peptides identified by LC–MS/MS and the proteins then classified according to their primary in vivo function, as stated by the UniProt database. Protein groups are expressed as a percentage of all protein identifications from corresponding peptides detected for each cycle. The number of positive identifications of a protein from its corresponding peptide was counted for each resin sample over all 120 fractions generated by LC.

Table 2
Common proteins detected from cycled resin samples. Note that this list does not reflect the number of times a protein was identified from its peptide fragments at each cycle; some proteins were detected in all/many of the different cycle samples but contributed little to the total number of peptide fragments detected. Keratin and trypsin variants were excluded from analysis due to their contaminant status.

Protein	Cycle number				Functional Class
	50	60	80	100	
Actin, cytoplasmic 1	+	+	+	+	Cytoskeletal
Actin-18	+	+	+	+	Cytoskeletal
DNA-directed RNA polymerase subunit omega	+	+	+	+	Protein synthesis
Elongation factor 2	+	–	+	+	Protein synthesis
Elongation factor Tu	–	+	+	+	Protein synthesis
Glyceraldehyde-3-phosphate dehydrogenase	–	+	+	+	Metabolism
Ig gamma-1 chain C region	+	+	+	+	*IgG*
Ig heavy chain V region 6.96	+	+	+	+	*IgG*
Ig heavy chain V region 914	+	+	+	+	*IgG*
Ig heavy chain V region MOPC 21	+	+	+	+	*IgG*
Ig kappa chain C region	+	+	+	+	*IgG*
Ig kappa chain V-I region AG	+	+	+	+	*IgG*
Ig kappa chain V-I region DEE	+	+	+	+	*IgG*
Protein A	+	+	+	+	Resin ligand
Kinetoplast-associated protein 1	+	+	+	–	Histone protein
Probable endonuclease 4	+	+	+	+	Protein synthesis

4. Conclusion

A relationship is reported between the appearance of surface deposits (foulants), reduction in resin capacity and the increase in the number of host cell proteins carried over between cycles of agarose based protein A chromatography. This was seen without significant impact on the critical quality attributes of HCP and protein A leachate levels in the eluate. The relationship is non-linear; the composition of the protein cohort remaining on the resin surface evolves, with a decreasing proportion of mAb and a concomitant increase in HCPs with cytoskeletal, protein synthesis and metabolism related proteins comprising a major proportion of the carried-over HCP. The data shows that, under these conditions, there is between 60 and 80 cycles a critical point after which the number of HCPs retained on the resin increases dramatically.

The increase in residual HCP, while a concern and associated with reduced DBC, was not associated with a loss in product quality. This indicates that the operation is robust. However, being able to monitor the accumulation of residual HCP would be of clear benefit to industrial processes, to understand and mitigate any risk residual HCPs might present [3,27]. Development of a non-invasive method to monitor the accumulation of residual HCPs would provide an early prediction of when a column is approaching the end of its lifetime, preventing operational faults before they manifest.

Acknowledgements

The authors wish to thank Mark Turmaine at UCL electron microscope facility for valuable advice with SEM procedures. We are grateful to the EPSRC for providing the grant necessary to conduct this research ("Creation of a process understanding of chromatographic performance loss during biotherapeutics manufacture", a UK-India partnership (EP/K029053/1).

References

[1] H.F. Liu, J. Ma, C. Winter, R. Bayer, Recovery and purification process development for monoclonal antibody production, mAbs 2 (2010) 480–499.
[2] W.S. Putnam, S. Prabhu, Y. Zheng, M. Subramanyam, Y.M.C. Wang, Pharmacokinetic, pharmacodynamic and immunogenicity comparability assessment strategies for monoclonal antibodies, Trends Biotechnol. 28 (2010) 509–516.
[3] D.G. Bracewell, R. Francis, C.M. Smales, The future of host cell protein (HCP) identification during process development and manufacturing linked to a risk-based management for their control, Biotechnol. Bioeng. 112 (2015) 1727–1737.
[4] C.E. Hogwood, A.S. Tait, N. Koloteva-Levine, D.G. Bracewell, C.M. Smales, The dynamics of the CHO host cell protein profile during clarification and protein A capture in a platform antibody purification process, Biotechnol. Bioeng. 110 (2013) 240–251.
[5] N.E. Levy, K.N. Valente, L.H. Choe, K.H. Lee, A.M. Lenhoff, Identification and characterization of host cell protein product-associated impurities in monoclonal antibody bioprocessing, Biotechnol. Bioeng. 111 (2014) 904–912.
[6] A.A. Shukla, P. Hinckley, Host cell protein clearance during protein A chromatography: development of an improved column wash step, Biotechnol. Progress 24 (2008) 1115–1121.
[7] N. Aboulaich, W.K. Chung, J.H. Thompson, C. Larkin, D. Robbins, M. Zhu, A novel approach to monitor clearance of host cell proteins associated with monoclonal antibodies, Biotechnol. Progress 30 (2014) 1114–1124.
[8] E.J. Close, J.R. Salm, T. Iskra, E. Sorensen, D.G. Bracewell, Fouling of an anion exchange chromatography operation in a monoclonal antibody process: visualization and kinetic studies, Biotechnol. Bioeng. 110 (2013) 2425–2435.
[9] J. Jin, S. Chhatre, N.J. Titchener-Hooker, D.G. Bracewell, Evaluation of the impact of lipid fouling during the chromatographic purification of virus-like particles from Saccharomyces cerevisiae, J. Chem. Technol. Biotechnol. 85 (2010) 209–215.
[10] P. Gagnon, R. Nian, J. Lee, L.H. Tan, S.M.A. Latiff, C.L. Lim, C. Chuah, X.Z. Bi, Y.S. Yang, W. Zhang, H.T. Gan, Nonspecific interactions of chromatin with immunoglobulin G and protein A, and their impact on purification performance, J. Chromatogr. A 1340 (2014) 68–78.
[11] P. Gagnon, R. Nian, L. Tan, J. Cheong, V. Yeo, Y. Yang, H.T. Gan, Chromatin-mediated depression of fractionation performance on electronegative multimodal chromatography media, its prevention, and ramifications for purification of immunoglobulin G, J. Chromatogr. A 1374 (2014) 145–155.
[12] S. Zhang, W. Daniels, J. Salm, J. Glynn, J. Martin, C. Gallo, R. Godavarti, G. Carta, Nature of foulants and fouling mechanism in the protein A MabSelect resin cycled in a monoclonal antibody purification process, Biotechnol. Bioeng. 113 (2016) 141–149.
[13] S. Zhang, K. Xu, W. Daniels, J. Salm, J. Glynn, J. Martin, C. Gallo, R. Godavarti, G. Carta, Structural and functional characteristics of virgin and fouled protein A MabSelect resin cycled in a monoclonal antibody purification process, Biotechnol. Bioeng. (2015).
[14] C. Jiang, J. Liu, M. Rubacha, A.A. Shukla, A mechanistic study of Protein A chromatography resin lifetime, J. Chromatogr. A 1216 (2009) 5849–5855.
[15] A. Gronberg, M. Eriksson, M. Ersoy, H.J. Johansson, A tool for increasing the lifetime of chromatography resins, mAbs 3 (2011) 192–202.
[16] A.S. Rathore, M. Pathak, G.J. Ma, D.G. Bracewell, Re-use of protein A resin: fouling and economics, Biopharm. Int. 28 (2015) 28–33.
[17] S.S. Farid, Process economics of industrial monoclonal antibody manufacture, J. Chromatogr. B 848 (2007) 8–18.
[18] R. Hahn, K. Shimahara, F. Steindl, A. Jungbauer, Comparison of protein A affinity sorbents III. Life time study, J. Chromatogr. A 1102 (2006) 224–231.
[19] C.S. Burden, J. Jin, A. Podgornik, D.G. Bracewell, A monolith purification process for virus-like particles from yeast homogenate, J. Chromatography. B 880 (2012) 82–89.
[20] J.N. Carter-Franklin, C. Victa, P. McDonald, R. Fahrner, Fragments of protein A eluted during protein A affinity chromatography, J. Chromatogr. A 1163 (2007) 105–111.
[21] H. Dorai, A. Santiago, M. Campbell, Q.M. Tang, M.J. Lewis, Y. Wang, Q.Z. Lu, S.L. Wu, W. Hancock, Characterization of the proteases involved in the N-terminal clipping of glucagon-like-peptide-1-antibody fusion proteins, Biotechnol. Progr. 27 (2011) 220–231.
[22] H. Sandberg, D. Lutkemeyer, S. Kuprin, M. Wrangel, A. Almstedt, P. Persson, V. Ek, M. Mikaelsson, Mapping and partial characterization of proteases expressed by a CHO production cell line, Biotechnol. Bioeng. 95 (2006) 961–971.
[23] S.X. Gao, Y. Zhang, K. Stansberry-Perkins, A. Buko, S. Bai, V. Nguyen, M.L. Brader, Fragmentation of a highly purified monoclonal antibody attributed to residual CHO cell protease activity, Biotechnol. Bioeng. 108 (2011) 977–982.
[24] A. Farrell, S. Mittermayr, B. Morrissey, N. Mc Loughlin, N. Navas Iglesias, I.W. Marison, J. Bones, Quantitative host cell protein analysis using two dimensional data independent LC–MS(E), Anal. Chem. 87 (2015) 9186–9193.
[25] K. Mihara, Y. Ito, Y. Hatano, Y. Komurasaki, A. Sugimura, M. Jones, H. Liu, S. Mai, O. Lara-Velasco, L. Bai, A. Ketkar, M. Adams, T. Hirato, R. Ionescu, Host cell proteins: the hidden side of biosimilarity assessment, J. Pharm. Sci. (2015).
[26] C.E. Doneanu, M. Anderson, B.J. Williams, M.A. Lauber, A. Chakraborty, W. Chen, Enhanced detection of low-abundance host cell protein impurities in high-purity monoclonal antibodies down to 1 ppm using ion mobility mass spectrometry coupled with multidimensional liquid chromatography, Anal. Chem. 87 (2015) 10283–10291.
[27] C.L. de Zafra, V. Quarmby, K. Francissen, M. Vanderlaan, J. Zhu-Shimoni, Host cell proteins in biotechnology-derived products: a risk assessment framework, Biotechnol. Bioeng. 112 (2015) 2284–2291.